Proceedings of ASME Turbo Expo 2015
GT2015
June 15-19, 2015, Montreal, Canada

GT2015-44140

HARMONIC CONVERGENCE ESTIMATION THROUGH STRAIN ENERGY SUPERCONVERGENCE

Alexander A. Kaszynski
Universal Technology Corporation
Dayton, OH 45434
Email: akascap@gmail.com

Joseph A. Beck
Jeffrey M. Brown
Turbine Engine Division
U.S. Air Force Research Laboratory
Wright-Patterson AFB, OH 45431

ABSTRACT

Grid convergence in finite element analysis, despite a wide variety of tools available to date, remains an elusive and challenging task. Due to the complex and time consuming process of remeshing and solving the finite element model (FEM), convergence studies can be part of the most arduous portion of the modeling process and can even be impossible with FEMs unassociated with CAD. Existing a posteriori methods, such as relative error in the energy norm, provide a near arbitrary indication of the model convergence for eigenfrequencies. This paper proposes a new approach to evaluate the harmonic convergence of an existing model without conducting a convergence study. Strain energy superconvergence takes advantage of superconvergence points within a FEM and accurately recovers the strain energy within the model using polyharmonic splines, thus providing a more accurate estimate of the system's eigenfrequencies without modification of the FEM. Accurate eigenfrequencies are critical for designing for airfoil resonance avoidance and mistuned rotor response prediction. Traditional error estimation strategies fail to capture harmonic convergence as effectively as SES, potentially leading to a less accurate airfoil resonance and rotor mistuning prediction.

NOMENCLATURE

DOF	Degrees of freedom
FE	Finite element
FEA	Finite element analysis
FEM	Finite element model
IBR	Integrally bladed rotor
RBF	Radial basis function
PRERR	Percent error in the energy norm
PSIM	Polyharmonic spline interpolation method
SERR	Strain energy error
SES	Strain energy superconvergence
SPR	Superconvergent patch recovery
ω_n	Natural frequency

INTRODUCTION

At its core, the finite element method is a computational approach to discretize a field problem to estimate the solution of its field variables and the derivatives thereof [1]. In structural analysis the field is the geometric volume V, the finite element domain is V_h, and the primary field variable is displacement u. The finite element domain V_h consists of cell-wise polynomial shape functions of order p and is commonly referred to as the finite element model (FEM). These polynomial functions and the FEM in general are merely a numerical approximation of the true solution resulting in inherent modeling error. The focus of this paper will be the estimation of the error of the eigensolution to

$$[\mathrm{M}]\ddot{u} + [\mathrm{K}]u = \mathrm{F} \tag{1}$$

where [M] is the mass matrix and [K] is the stiffness matrix, and both dependent on the aforementioned piecewise element-based

shape functions. This paper will assume an unforced solution of the eigensystem and therefore force F will be considered null. The solution of the eigenproblem yields a set of eigenvalues representative of the system's natural frequencies and a set of eigenvectors that correspond to the mode shapes of the system. Utilizing the assumption that each of these mode shapes is linear, the displacement of a single node in the FEM will yield proportional displacements to the rest of the FEM according to the eigenvector (mode shape).

The finite element method is used in the engine design process to estimate airfoil mode shapes, natural frequencies, and is crucial for determining safe engine operating ranges. Particularly for integrally bladed rotors (IBRs), accurate natural frequencies and mode shapes are necessary for determining the mistuned forced response which may lead to catastrophic blade failure from high cycle fatigue (HCF) [2]. For IBRs, where 10^{-1} % error in blade alone natural frequencies is sufficient for a poor mistuning prediction, minimizing model error is essential [3].

There are several sources of errors within an FEM including user-induced errors such as poorly modeled boundary conditions, inaccurate geometry or CAD, discretization error, and interpolation error [4]. The first two are caused by a failure to accurately represent the physical world in the digital domain and are specific to individual models, while interpolation and discretization error must be considered in every FEA. Interpolation error arises mainly from the relationship between the ideal element shape and the actual element shape as defined by the Jacobian and formulated as an element shape function with FEA. Element shape functions can be inaccurate for highly distorted elements, contribute to interpolation error, and lead an inaccurate matrices of the eigenproblem. While there exists tremendous research regarding element shape validity and its effect on the finite element (FE) solution, to date no element shape test can effectively generate an error bound for either stress or eigenfrequency accuracy, only existing discontinuities [5].

To begin development of an eigenfrequency error bound method, we consider the mesh discretization error. Discretization error is an inherent systemic problem arising from the discrete nature of the finite element subspace. This error is of the form

$$a(e_h, v_h) = a(u, v) - a(u_h, v) \tag{2}$$

where e_h is the error of the finite element solution, v is the location in the FEM subspace, and u is the first field variable (displacement) of the eigenproblem. As with interpolation error, there are no algorithms to directly compute an error bound on either the primary or secondary field derivatives resulting from the solution of the eigenproblem. Indirectly, an analyst can conduct a mesh convergence study to observe the variation in the eigensolution while global or local element edge length is varied. A mesh convergence study is in general a challenging and time consuming task. The analyst can have difficulties regenerating the FE mesh over the field domain and may encounter memory limitations or long solution times during the process. Because of these challenges, convergence studies are frequently avoided or truncated, leaving the engineer with a blind confidence on the results from commercial 'Black Box' FE codes [6]. Ideally, there would exist an error estimator that yields the approximate error in the eigensolution that is rapidly computable and straightforward to employ.

This paper advances and refines a novel *a posteriori* technique to estimate harmonic convergence without modifying an existing FEM. Strain energy superconvergence (SES) recovers element strain energy to compute more accurate eigenfrequencies for modes of interest. This method extends research conducted by Baušys in *Accuracy Estimates in Free Vibration Analysis* [7] by employing polyharmonic splines to more accurately interpolate the displacement field using element superconvergence points. It will be shown that SES computes a more accurate system natural frequency estimate regardless of element shape and density, thereby capturing both interpolation and discretization error.

The paper begins with a review of existing error estimation techniques and their flaws. Then, the relationship between strain energy and system natural frequency is developed and exploited using smoothed displacement fields from various interpolation methods, including polyharmonic splines. These various approaches are then applied to academic cantilever beams and various complex FEMs, including an IBR sector model, to demonstrate the fidelity and accuracy of the SES technique.

CURRENT ERROR ESTIMATION TECHNIQUES

Error in energy norm is an established *a posteriori* error estimation tool which accounts for the discontinuity of strain across element boundaries [8]. As each element shape function is only valid for its corresponding cell, element shape functions are discontinuous over the entire field domain. Strain within a finite element is a function of

$$\boldsymbol{\varepsilon}^e = [\mathrm{B}^e]\{u^e\} \tag{3}$$

given element shape function $[\mathrm{B}^e]$ and the displacements u^e of the nodes composing the element e. While the global system may contain a continuous solution of displacements from the solution of the eigenproblem, strain is discontinuous as the element shape function is piecewise discontinuous. Discontinuities in the system strain field indicate that the elements composing the system misrepresent the underlying global system as they contribute to the formulation of the strain matrix and hence the eigensolution. One error estimation approach is to measure the error between a smoothed strain field and the actual strain field to measure strain discontinuity. This is accomplished by first comput-

ing the strain at each node for each element by evaluating the shape matrix $[B^e]$ at the ideal Gauss-quadrature points and then extrapolating to the corner nodes. While strain can be computed directly at a node within an element without the utilization of Gauss points, a more accurate solution can be obtained by using Gauss-quadrature points and extrapolating the strain computed at the Gauss points to the nodes of an element. For example, in a 2D quadrilateral element, the shape function is of the form

$$\mathrm{B} = \begin{bmatrix} \frac{\partial x_1}{\partial s} & 0 & \frac{\partial x_2}{\partial s} & 0 & \frac{\partial x_3}{\partial s} & 0 & \frac{\partial x_4}{\partial s} & 0 \\ 0 & \frac{\partial y_1}{\partial t} & 0 & \frac{\partial y_2}{\partial t} & 0 & \frac{\partial y_3}{\partial t} & 0 & \frac{\partial y_4}{\partial t} \\ \frac{\partial x_1}{\partial s} & \frac{\partial y_1}{\partial t} & \frac{\partial x_2}{\partial s} & \frac{\partial y_2}{\partial t} & \frac{\partial x_3}{\partial s} & \frac{\partial y_3}{\partial t} & \frac{\partial x_4}{\partial s} & \frac{\partial y_4}{\partial t} \end{bmatrix} \tag{4}$$

where the partial derivative $\partial x_{\mathrm{n}}/\partial s$ is derived from the Jacobian that describes the transformation between the Cartesian coordinate system and the element coordinate system at node n. The Jacobian is evaluated at the four Gauss points $(\pm\sqrt{\frac{1}{3}},\pm\sqrt{\frac{1}{3}})$ and then used to the assemble the B matrix. The strain is then extrapolated from the Gauss points to the nodes. As each node generally belongs to more than one element, the relative strain error at each node can be computed via

$$\Delta\varepsilon_{e_n} = \varepsilon_{e_n} - \varepsilon_{\mathrm{a}_n} \tag{5}$$

where $\Delta\varepsilon_{\mathrm{e}}$ is the strain error at node n for element e and $\varepsilon_{\mathrm{a}_n}$ represents strain at node n. As the actual strain is an unknown, the actual strain $\varepsilon_{\mathrm{a}_n}$ at node n for Equation 5 is estimated by averaging the individual strain solution from multiple elements using a volume weighted scheme. Having computed the nodal strain error from the smoothed strain, the strain error is then integrated over each corresponding element using

$$\mathrm{SE}_e = \int \Delta\varepsilon_e[\mathrm{C}]\Delta\varepsilon_e^{\mathsf{T}}\,dA \tag{6}$$

such that SE_e is the strain energy error at element e, $\Delta\varepsilon_e$ is the nodal strain error over the element e, and [C] is the stress-strain constitutive matrix. The solution is computed by Gaussian quadrature numeric integration and is the sum of the strain solution at the Gauss points within the element multiplied by the total area of the element. The strain energy error is then summed for the entire model and normalized by the total strain energy of the FEM in

$$E = 100\sqrt{\frac{\mathrm{SE}_e}{\mathrm{SE}_e + \mathrm{SE}}} \tag{7}$$

in which SE_e is the sum of the strain energy error in the FEM and SE sum of the strain energy in the FEM for a given mode shape. This ratio is known as the percent error in energy norm (PRERR) and is used to estimate the error in the modal solution based on the assumption that a large jump in strain across an element boundary indicates a poor approximation of the local

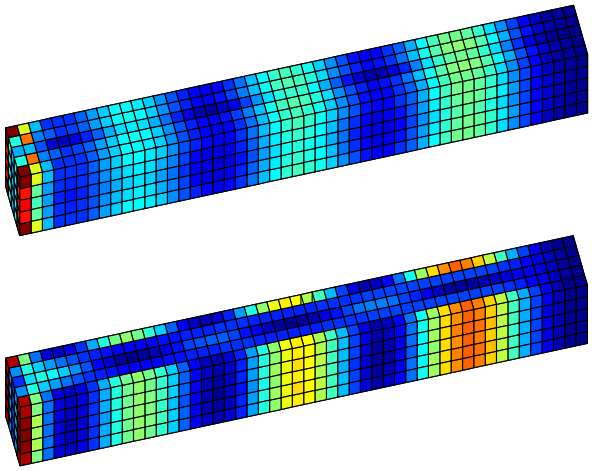

FIGURE 1. Cantilever Beam Strain Energy Error (Top) and Strain Energy (Bottom)

element shape functions and indicates that there is error in the FEA solution.

To illustrate this a $5 \times 0.5 \times 0.5$ meter cantilever beam was meshed using 8-node trilinear hexahedral elements and a convergence study was conducted on it by varying the mean edge length of the elements while maintaining a uniform distribution of equilateral hexahedrons throughout the beam. Figure 1 shows the strain energy and strain energy error for the beam, and as expected the largest discontinuity in strain energy is at the wall boundary condition and where there is a large concentration of strain energy. The strain energy error (SERR) and percent deviation from an analytical prediction of the natural frequency of the beam are shown in Figure 2 for the third bending mode. For this particular FEM, SERR appears to be an excellent indicator of eigenfrequency convergence. The approximate relationship

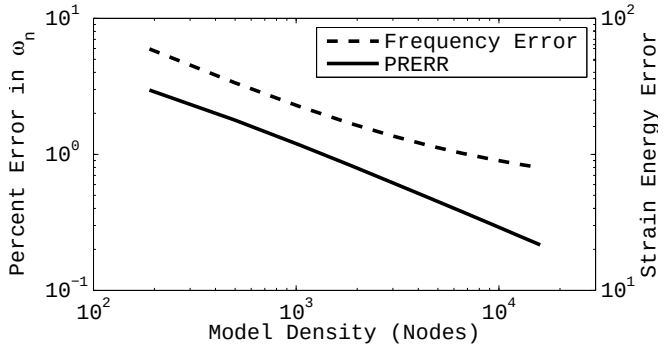

FIGURE 2. Strain Energy Error and Frequency Error with Respect to Nodal Density

between the solution's discrepancy from the analytical solution and the error in strain energy is unity when PRERR is treated as a ratio rather than a percentage.

Despite this good result, varying the geometry of the cantilever beam results in a completely different relationship between the error in strain energy and frequency error. A second cantilever beam was generated with dimensions approximating the geometry of an upper stage fan blade whose geometry can be observed in Figure 3. With no analytical solution for the twisted beam, a second FEM utilizing quadratic hexahedral elements was solved and converged for the 3rd bend natural frequency to seven significant figures. Referring to the results in Figure 4, while the strain energy error and frequency error correlate, the ratio between them is neither constant nor similar to the original beam model. The jagged behavior in the frequency error is caused by the varying aspect ratio across the twisted cantilever beam and this is not reflected in the strain energy error. This behavior is also exhibited in an even greater degree for the first three torsional modes of this beam, though these results have been excluded from Figure 4 for clarity. These results indicate that strain energy error can be insensitive to element interpolation error.

While SERR can be used to as a reasonable estimate of potential stress error given strain discontinuities [9], SERR is not a reliable indicator of harmonic convergence as it cannot consistently predict eigensolution convergence. This is mainly due to the fact that strain discontinuity across elements is a derivative of a field value and is only indirectly related to the eigenfrequencies from the eigensolution. With a lack of an accurate harmonic convergence estimation tool the engineer is left with two choices: either utilize a *a posteriori* error indicator more suited to stress convergence, or to conduct a time consuming convergence study to determine eigenfrequency convergence. Though this convergence study may be automated by certain *a posteriori* mesh refinement techniques based on strain energy error which have

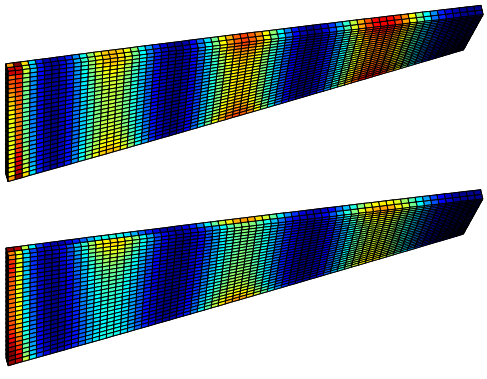

FIGURE 3. Twisted Canteliver Beam Strain Energy in 3B

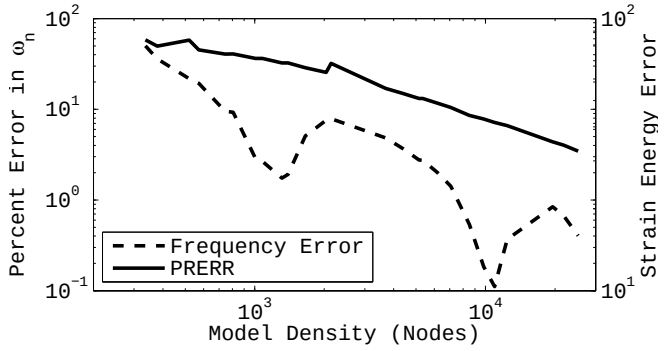

FIGURE 4. Strain Energy Error and Frequency Error for Twisted Cantilever Beam

been implemented for certain classes of elements (e.g. tetrahedrals) [10], an automated hexahedral refinement processremains an unsolved problem. Additionally, these techniques focus solely on stress and not eigenfrequency convergence. Instead, an ideal solution would be an algorithm that could provide the engineer with an immediately computable estimate of frequency convergence invariant of the FEM's geometry, density, or quality. This paper proposes a new and straightforward method for obtaining and utilizing a smoothed displacement field to generate a more accurate eigenfrequency estimate and will be referred to henceforth as strain energy superconvergence (SES).

STRAIN ENERGY SUPERCONVERGENCE

The natural frequency of a mass spring system can be described as the ratio between the potential energy and the kinetic of the system. In terms of the FEM, this is the ratio of the strain energy to the mass energy for a given mode and is given below as the Rayleigh quotient

$$\omega_n^2 = \frac{\int \frac{1}{2}\varepsilon^{\intercal}\sigma dV}{\int \frac{1}{2}\rho \mathrm{u}^{\intercal}\mathrm{u} dV} \tag{8}$$

with strain ε and stress σ in the numerator and density ρ and nodal displacement u in the denominator. The Rayleigh quotient is computed by integrating the strain and mass energy over each element's volume V. Baušys in *Accuracy Estimates in Free Vibration Analysis* [7] showed that if one were to obtain a more accurate displacement field using an *a posteriori* recovery method it would be possible to recompute the Rayleigh quotient for the finite element model and more accurately estimate the eigenfrequency for a specific mode shape. However, for the interpolated displacement it must be sampled at the superconvergent displacement locations, which for Lagrangian elements are along the edge boundaries of the elements. The order and shape of the element (e.g. linear tetrahedral) determines the number

and location of the interpolation points within the interpolated displacement field. Equation 8 can then reevaluated using the recomputed strain, stress, and displacement values from the higher order elements, thus yielding a more accurate Rayleigh quotient and eigenfrequency for the mode of interest.

There are several approaches to interpolating the original displacement field. Baušys utilized the superconvergence patch recovery method in his research and applied it to 2D boundary free plates by using superconvergent optimal sampling points. The existence of optimal sampling points within the FEM has been suggested in early FEA research [11], and these optimal points are coincident with the reduced Gauss quadrature points. For example, the $1\times$ Gauss point would be used when 2×2 Gauss points would be necessary for the full integration of a quadrilateral element. The superconvergence patch recovery method (SPR) [12] is based on a local least squares optimization across discrete patches using field variables or their derivatives (e.g. displacement, strain, or stress) at the superconvergent points. For each patch it is assumed the values at each superconvergent point belong to a polynomial expansion of the same order p present in the shape functions composing the element. This polynomial expression is

$$u_p = \mathrm{P}a \tag{9}$$

where u_p is the displacement of each superconvergent point, P is the set of appropriate polynomial terms, and a is a set of parameters relating the two. For the bilinear quadrilateral elements to be used in this example the polynomial terms are

$$\mathrm{P} = [1, x, y, xy] \tag{10}$$

where x and y are the physical coordinates of an existing sampling point. The parameter set a then is solved for by summing the contributions of each superconvergence point in

$$A = \sum_{i=1}^{n} \mathrm{P}^{\mathsf{T}}(x_i, y_i) P(x_i, y_i)$$

$$b = \sum_{i=1}^{n} \mathrm{P}(x_i, y_i) u_h(x_i, y_i)$$

and enforcing a least squares fit by solving

$$a = A^{-1} b \tag{11}$$

The displacements at the new locations are then interpolated from Equation 9 using the coefficients from Equation 11 and these displacements are then used to recompute the potential and kinetic energy of each element for use in the Rayleigh quotient. Recall that the original strain energy was computed using an individual element solution where the shape matrix [B] was evaluated at the Gauss-quadrature points and was multiplied by the nodal displacement vector u to compute the strain at that point. This strain energy was then numerically integrated over the element by summing the strain at the Gauss points and multiplying the result by either the area or volume of the element depending on the dimensional order of the element. The new displacement field is utilized in much of the same manner: the displacements interpolated at the higher order sampling points is interpolated using Gauss-quadrature and then numerically integrated over the element.

Alternatively, instead of computing strain energy from shape functions based on an interpolated displacement field, another approach would be to directly compute element strain energy using the node averaged strain from an element volume weighted averaging scheme. As cited in research by Zienkiewicz in [12], the nodal averaging of field derivatives, including strain, has been practiced since the beginning of the FE method to provide the user with more assessable smoothed results, and the effectiveness of this method is largely due to its loose relationship to superconvergence points. A more rapid, non-patch based interpolation approach would be to use averaged nodal strains and then locally interpolate from these nodal strains within an element using Gaussian quadrature. This approach will be compared to Baušys's work.

A numerical study of both the SPR and nodal averaging approaches was conducted on a 2D 0.5×5 meter beam which was meshed with 2D bilinear quadrilateral elements restricted to the planar displacements $\mathrm{u_x}$ and $\mathrm{u_y}$. A zero displacement boundary condition was implemented at the left most edge and the analytical solution was computed using an accepted wall fixed cantilever beam equation [13]. A convergence study was conducted on this mesh by varying the mean element edge length while maintaining ideal equilateral element shape to eliminate interpolation error and limit the analysis to discretization error. The results of the convergence study are reported in Figure 5, which indicates the convergence rate of the unmodified mesh is unity on a log-log scale, whereas the SPR based displacement interpolation method achieves an order of magnitude greater accuracy while still maintaining a log-log relationship. Given that the convergence rate between element size and frequency error generally have log-log relationship [8], Baušys's approach appears to be accurate for cantilever beams, and these results are similar to his original research. Additionally, averaged strain energy interpolation also appears to provide an accurate eigenfrequency estimation.

However, the variation between the original mode shape strain energy for 1^{st} bend (1B) and the results from the convergence study reveals a potential flaw in the nodal averaged strain approach. Figure 6 shows that elements on the boundaries of the FEM have a consistently smaller variation in strain energy than their internal counterparts in the nodal averaging approach, and this is due to the lack of exterior elements that would provide

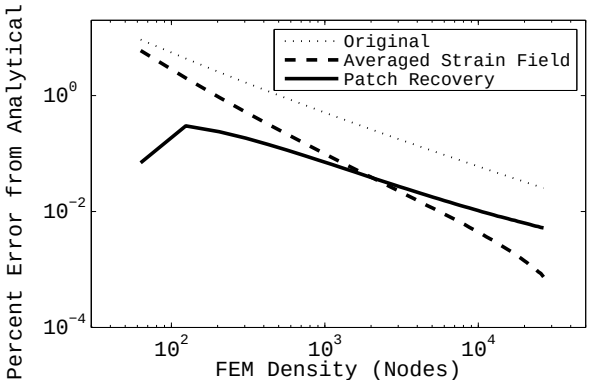

FIGURE 5. Improved Eigenfrequency Estimation Comparison

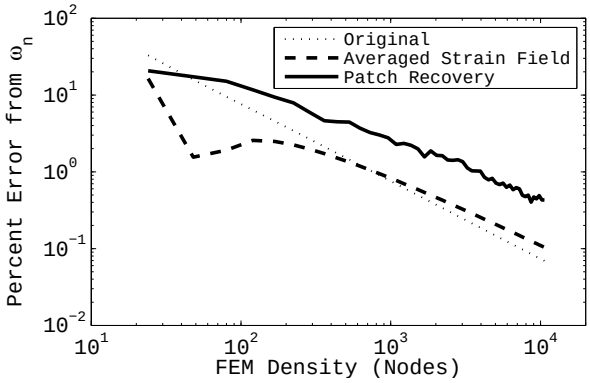

FIGURE 7. Annulus Recovered Strain Energy Variation

more accurate strain estimates at the exterior nodes of the FEM. SPR avoids this problem by extrapolating the strain from the interior superconvergence points to the exterior nodes of the FEM. The higher convergence rate of the nodal averaging scheme is actually an artifact caused by the lower strain energy due to the underestimation of strain energy at exterior elements.

While Baušys's original research can provide a more accurate eigenfrequency estimate for 2D plates, this method has yet to be applied beyond simple structures to more complex geometries or higher dimensional elements. Using Baušys's algorithm a convergence study was conducted on a boundary free 2D annulus modeled with bilinear quadrilaterals by varying the mean element edge length, and as indicated in Figure 7, neither the strain averaging scheme nor the patch recovery method provide a more accurate eigenfrequency estimate for this new geometry. The weakness of SPR is highlighted in Figure 8 where the patch recovery method shows numerical instability due to the quasi-uniformity of the FEM and particularly due to the rank deficiency of the interpolation matrix [A], both of which are established problems of SPR for linear and bilinear elements [14, 15]. While this is indicative of the challenges of utilizing SPR, it does not indicate that the reevaluation of the Rayleigh quotient is at fault, merely the interpolation approach.

While numerous improvements to the SPR method have been proposed by various authors in [16,17], it will be shown that the more optimal approach is to utilize polyharmonic spline interpolation to avoid matrix ill-conditioning and to compute more accurate results than SPR.

POLYHARMONIC SPLINE INTERPOLATION APPLIED TO SES

Polyharmonic splines are an interpolation method well suited to scattered data in multiple dimensions. One advantage of

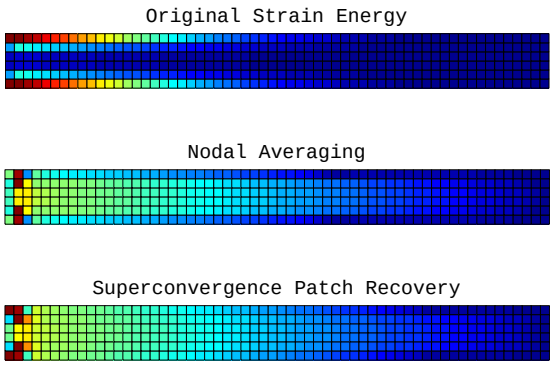

FIGURE 6. Recovered Strain Energy Variation

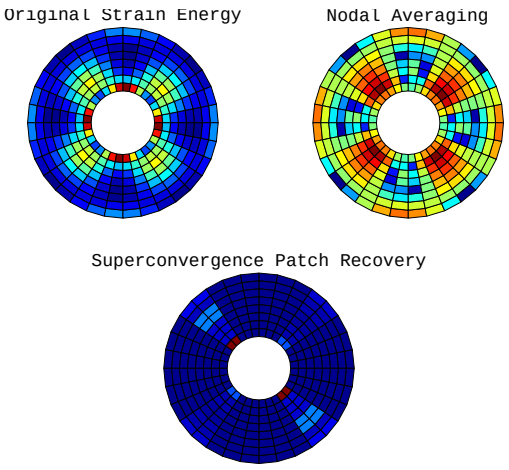

FIGURE 8. Annulus Eigenfrequency Estimation Comparison

the polyharmonic spline interpolation method is that data can be interpolated without tuning the coefficient matrix, unlike Gaussian radial basis functions in which nodal weighting needs to be finely adjusted to achieve an accurate fit through existing values. A polyharmonic spline is defined as

$$y(x) = \sum_{i=1}^{N} w_i \phi(\|x - c_i\|) + v^\intercal \begin{bmatrix} 1 \\ x \end{bmatrix} \tag{12}$$

where $x = [x_1, x_2, ..., x_{nx}]^\intercal$ is a real-valued vector of n independent variables, $c_i = [c_{1,i}, c_{2,i}, ..., c_{n,i}]^\intercal$ are n vectors of the same size as x and are the sampling locations of the independent variables in which the polyharmonic spline must pass through. Weights w and v are the weights of the basis functions and the polyharmonic spline, respectively. These weights are determined by solving the symmetric linear system of equations

$$\begin{bmatrix} A & V^\intercal \\ V & 0 \end{bmatrix} \begin{bmatrix} w \\ v \end{bmatrix} = \begin{bmatrix} y \\ 0 \end{bmatrix} \tag{13}$$

where

$$0 = \sum_{i=1}^{N} w_i, \;\; 0 = \sum_{i=1}^{N} w_i c_{j,i}$$

$$A_{i,j} = \phi(\|c_i - c_j\|)$$

$$V = \begin{bmatrix} 1 & 1 & \cdots & 1 \\ c_1 & c_2 & \cdots & c_n \end{bmatrix}$$

$$y = [y_1, y_2, \cdots, y_n]^\intercal$$

in which $\|c_i - c_j\|$ describes the distance between center c_i and all other centers c_j, and y_n is the value to be interpolated at the center n while the weights are constrained such that the weights and product of the weights and intra-center distances sum to zero. The radial basis function $\phi(r)$ is

$$\phi(r) = \begin{cases} r^{k-1}\ln(r^r) & \text{if } k \text{ is odd} \\ r^k \ln(r) & \text{if } k \text{ is even} \end{cases} \tag{14}$$

in which k can be considered the order of interpolation (e.g. $k = 2$ is a second order polyharmonic interpolation) and an even order polyharmonic RBF must be multiplied by $\ln(r)$ to ensure the spline passes through the input centers. To apply the polyharmonic approach to the problem at hand, Equation 13 is solved using the displacements from the original FEM analysis and the RBF weights are computed for Equation 14, at which the new interpolation locations (i.e. node locations for the next higher order element) can be inputted into Equation 12 as x in

$$r = \|x - c\|_2 = \sqrt{(x - c_i)^\intercal (x - c_i)} \tag{15}$$

where c is an existing node of the original FEM and x is the new interpolation location. This interpolation method is similar to SPR such that the interpolation space is computed from existing values and locations, but different in that the polyharmonic spline method utilizes a global rather than local approach for determining weight coefficients.

Polyharmonic strain energy superconvergence was implemented for the same cantilever beam used in the earlier numerical test correlating strain energy error with frequency convergence. Linear tetrahedral elements were used rather than their hexahedral counterparts in order to demonstrate the effectiveness of SES despite the unstructured nature of tetrahedral meshes. This will demonstrate that SES is insensitive to discretization error as well as interpolation error. The volumetric FE mesh was generated using commercial mesh generation software and solved using linear constant strain tetrahedrals. The displacement at the nodes was then outputted and interpolated at newly introduced mid-side nodes using the polyharmonic spline method over the entire FEM. The existing displacements of the edge nodes was combined with the interpolated displacements at the mid-side nodes and element strain and mass energy was recomputed using Equation 8 and a new natural frequency was computed for the model.

Results from the convergence study in Figure 9 indicate the polyharmonic SES implementation yielded nearly an order of magnitude increase in frequency convergence over the original linear tetrahedral model. SES in this implementation is a valid *a posteriori* error estimation scheme given the log-log relationship between mean element edge length (inverse of nodal density) and the percent error from the analytical solution to the beam. Addi-

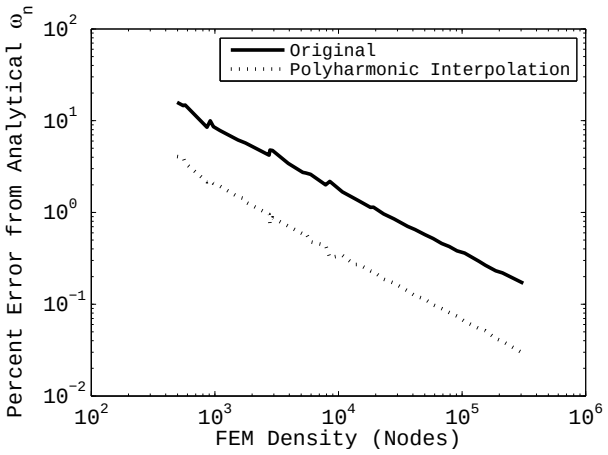

FIGURE 9. Tetrahedral FEM Convergence Study Results

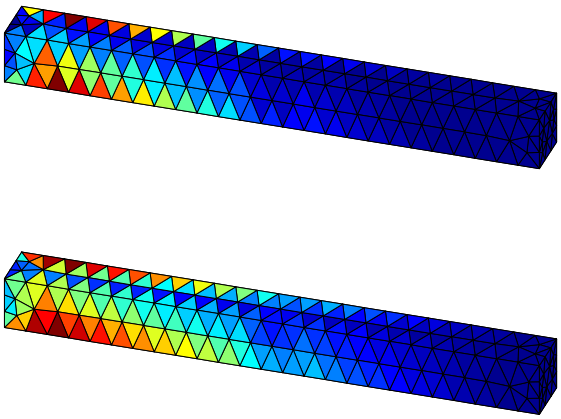

FIGURE 10. Strain Energy in Original Beam (Top) and Polyharmonic Interpolated Beam (Bottom)

tionally, it can be visually verified that the strain energy is more distributed and consistent given the results in Figure 10. The near order of magnitude improvement in eigenfrequency accuracy would have required the same order of magnitude increase in FEM density for the linear model and $O(10^2)$ increase in computation time.

However, while the polyharmonic spline interpolation method (PSIM) effectively eliminates weight matrix ill-conditioning and rank deficiency found in the SPR, it is computationally inefficient for large degree of freedom (DOF) systems as the weights must be solved for by inverting the non-sparse matrix on the left-hand side of Equation 13. This requires $\mathrm{O}(n^3)$ operations to solve the global system for n nodes as opposed to the $e\mathrm{O}(n_e^3)$ operations to solve e local systems with n_e nodes per local system as in SPR. The polyharmonic spline weight matrix is full rather than sparse and solving it is more computationally expensive than solving the actual FEM. This is the reason for the maximum 3×10^5 node limit to the convergence study. As modern FEMs can contain 10^6 or greater FEM nodes, a workaround is necessary to implement PSIM for large FEMs in a computationally efficient manner.

Clustered PSIM

Research by Beatson [18] shows that polyharmonic splines can be rapidly evaluated by avoiding full global interpolation when employing hierarchical methods to limit computational requirements and solution time. Their research was indirectly employed by regionally interpolating the FEM in order to break down the interpolation into smaller, more computationally feasible pieces. One approach would be to generate a PSIM "cloud" centered at an interpolation point (a midside node) of a reasonable size for to allow for sufficient interpolation accuracy. This approach was tested by varying the size of an interpolation field for three tetrahedral cantilever beam models similar to the model shown in Figure 10. The results in Figure 11 show that a surprisingly large interpolation cloud is necessary for high accuracy, far greater than the 8 - 20 neighbors that would be used by the SPR method for an unstructured tetrahedral FEM. As interpolation error directly correlates to error in eigenfrequency approximation it is necessary to utilize a large interpolation cloud of approximately 10^3 nodes to maintain eigenfrequency estimation accuracy within 6 significant figures. While the inversion of a single full $10^3 \times 10^3$ matrix is trivial, the inversion of $n \times 10^3 \times 10^3$ full matrices, where n is the number of new mid-side interpolation points, is as computationally infeasible as inverting a full weight matrix for global polyharmonic interpolation Instead, a better approach would be to generate multiple interpolation clusters in order to sequentially interpolate the FEM displacement field.

A cluster based interpolation method segments a FEM into multiple groups of nodes in order to maintain interpolation accuracy while limiting the weight matrix size. Using the well-established k-means clustering approach [19], the FEM is divided into adjacent and independent clusters whereby the interpolation weights are determined solely for that cluster. However, when implementing this approach it was discovered the resulting eigenfrequency estimates were less accurate than those obtained from global interpolation approach. This was verified by implementing clustered interpolation in a tetrahedral cantilever beam and comparing the interpolated mid-side node results from a 1000 element cluster to the global 20,000 node interpolation. Based on the accuracy scatter plot shown in Figure 12, the interpolation accuracy falls when moving away from the cluster center. It was discovered that the solution to this problem is to employ an overlapping cluster interpolation scheme to optimize

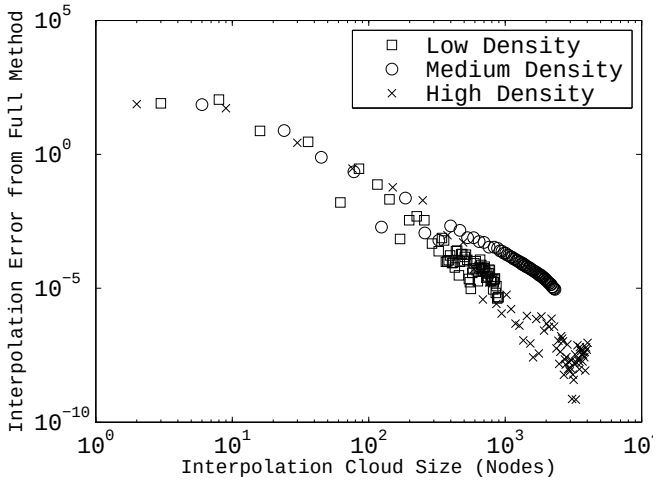

FIGURE 11. Interpolation Accuracy versus PSIM Cloud Size

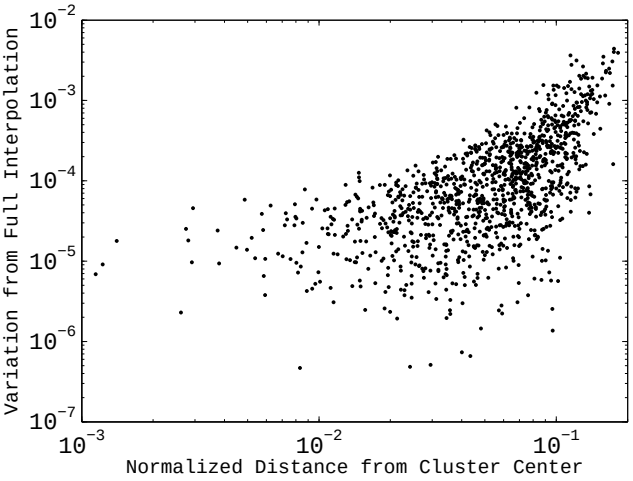

FIGURE 12. Interpolation Accuracy versus Distance to Cluster Center

solution accuracy by selecting the best interpolation results given multiple cluster of varying size and centers.

The optimal PSIM cluster scheme is effectively a three step process. First, a maximal cluster size is estimated based on available memory and optimal computing time. While smaller clusters limit the computational cost of inverting the PSIM cluster weight matrix, more clusters have to be solved. At some point, the computational cost of splitting, assembling, and looping through cluster arrays becomes more expensive than the inversion cost. For an Intel quad-core XEON computer running at 3.1 GHz with 32 GB RAM this occurred at a cluster size of approximately 5×10^4 nodes regardless of the size of the full model. Having computed the maximal cluster size, PSIM is then implemented on each cluster and the results of the interpolation are stored in a cell array for assembly. The final step is to decrease cluster size and to compute ideal cluster locations centered at nodes on the fringes of the previous cluster interpolation. This is repeated until the minimum nodal distance to a cluster center reaches a certain threshold, thus ensuring all nodes are within an optimal sampling distance without interpolating the global FEM.

The nodal results of the multi-cluster PSIM are combined based on an interpolation accuracy score. Nodal interpolation accuracy is based on cluster size and distance from the cluster center according to

$$a(n,c) = \mathrm{s}^{1-c}\frac{1-r_{nc}}{r_c} \tag{16}$$

where r_nc is the Euclidean distance between a node and its interpolation cluster center, r_c is the cluster size, and s^{1-c} is a solution accuracy weighting factor composed of the cluster size variation s and the current cluster iteration c. The interpolation results from multiple cluster iterations are combined such that the highest scoring node across all cluster interpolations is chosen and placed into a global interpolation result matrix. This implementation allows for a cluster size two orders of magnitude smaller than an non-iterative cluster interpolation while simultaneously achieving more accurate results for large DOF models.

Summarizing the clustered PSIM implementation for SES:

1. Solve the original FEM and output the eigenvalue and eigenvector for the mode of interest.
2. Add nodes to the original unmodified FEM at edge/surface superconvergence points corresponding to the next higher order element $(p+1)$.
3. Recompute the shape functions for the higher order element.
4. Cluster the FEM using k-means clustering and compute the polyharmonic weight matrix.
5. Interpolate within each cluster at the newly generated nodes using the weighting matrix from PSIM.
6. Modify the mean cluster size and rerun Step 4 while placing cluster centers on the fringes of the previous iteration's clusters. Repeat until the maximum node cluster score according to Equation 16 has reached a minimum specified threshold for all nodes.
7. Recompute the Rayleigh quotient using Equation 8 using the new shape matrices and interpolated displacements for the higher order elements. Output the updated eigenfrequency for the mode of interest.

Having demonstrated that clustered PSIM works for simplistic academic structures, it will be shown in the next two subsections that it can also be applied for FEMs generated from production hardware as well as unique and oddly shaped FEMs.

SES Implemented on a Production IBR Sector

The polyharmonic SES scheme was applied to a sector model from a production IBR to estimate eigenfrequency convergence given a convergence study. The sector model of the IBR was meshed with quadratic tetrahedrals with 10^6 nodes to generate the best approximation of a converged eigenfrequency. Boundary conditions were applied to the fore and aft surfaces of the bore and the FEM's nodal density was varied from approximately 10^4 to 5×10^5 nodes by varying the mean element edge length as in previous tetrahedral cantilever convergence studies. The results from Figure 13 indicate that SES provides nearly an order of magnitude increase in frequency accuracy for 1B despite the geometry complexity, boundary conditions, and inconsistent element density. Figure 14 shows the greatest change in strain energy occurs in the poorly shaped elements on the leading and trailing edges as well as the elements with the greatest strain energy. This indicates that SES is provides a more accurate estimate for poorly shaped elements and is therefore capable of accurately recovering interpolation error as well as discretization error.

More importantly, the clustered PSIM interpolation allowed for the interpolation of the model using polyharmonic splines without sacrificing accuracy due to potential low interpolation accuracy near the fringes of node clusters. The increase in accuracy at the blade leading and trailing edges indicates the cluster interpolation method is able to accurately recover interpolated displacements despite poor element shapes, thus demonstrating the robustness of the method despite the interpolation error from the original solution.

In the specific application to a geometrically mistuned IBR, SES can be used to determine blade-blade eigenfrequency variation due to mesh convergence as opposed to geometric variation between blades. Given the sensitivity of mistuning amplification

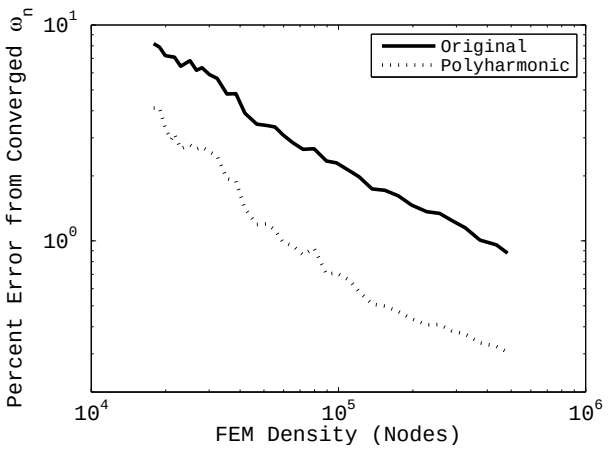

FIGURE 13. Production IBR SES Convergence Study

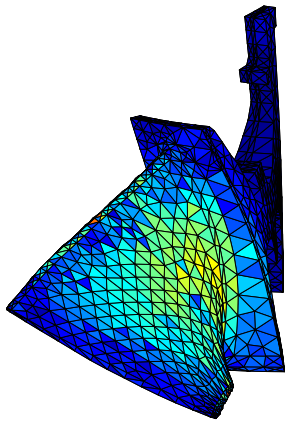

FIGURE 14. Recovered Strain Energy Variation in 1st Bend for a Production IBR Sector

due to blade-blade frequency variations, the accurate computation of blade alone frequency is crucial and SES can provide an error bound on frequency convergence by providing results from simulated and interpolated higher order elements without resolving, remeshing, or modifying the existing FEM in any manner.

It should be noted that mistuning amplification depends on the modal confinement of energy due to blades acting as tuned absorbers for system modes [20] and other system vibrational characteristics. Therefore, while the eigenfrequency results from SES may be more accurate, global mode shapes will be invariant as SES only interpolates from an existing the displacement field and does not modify existing known displacements. However, using SES the engineer can decide if the existing model is sufficiently accurate to predict mistuning amplification, or if poorly converged blade frequencies are nullifying the effects of actual geometric blade-blade mistuning. While the contribution that blade frequency variation has on mistuning results is debated in mistuning prediction [21], research indicates [3] that mistuning amplification is highly sensitive and minute variations in blade frequencies have a large contribution to the overall mistuned response. This reinforces the requirement for a converged FEM, and clustered PSIM can serve as an eigenfrequency convergence estimation scheme.

SES Implemented on an Incomplete Inflated Torus

Polyharmonic SES interpolation has been tested thus far on structures with beam dominant modes. To demonstrate that PSIM works for a variety of complex geometries and non-bending modes, PSIM has been implemented on an incomplete non-uniform inflated torus. The torus used for this analysis is shown in Figure 15 and is non-axis symmetric, has a varying wall thickness, and has two open ends. As in the previous analyses, this torus has been modeled with linear constant strain tetrahe-

drals and was interpolated with simulated quadratic tetrahedrals. This torus was also modeled without boundary conditions to test for possible weaknesses in the interpolation approach to include building the interpolation cloud from nearby disconnected nodes that might unduly influence the interpolation solution of the local cluster. This includes, but is not limited to, clusters large enough to include nodes from the disconnected ends of the inflated torus, as well as clusters including nodes from the entire cross section of the torus.

While the vibrational modes of the torus include in and out of plane bending modes, the torus exhibits several antisymmetric (twisting) modes. To capture these types of modes the first 19 modes of the torus were analyzed within FEA software and each mode was individually interpolated using clustered PSIM during the convergence study. As there was no straightforward analytical solution to this unusual structure, the converged solution was computed using a high density quadratic tetrahedral model containing approximately 5×10^5 nodes at which the eigenvalues for the modes of interest had been converged to six significant figures.

The results of the analysis shown in Figure 16 indicate that the PSIM approach consistently achieves a more accurate estimate for the first 19 eigenvalues of the model. It should be noted that neither the original nor the interpolation based eigenvalues follow a log-log relationship with the FEM density, indicating that mesh convergence for this type of structure is more difficult to achieve and this is likely due to the convex geometry of both the wall and the torus itself. Coarse meshes utilizing linear elements will cause both interpolation error as well geometric approximation error as the piecewise linear geometry of the individual elements do not follow the curvature of the geometric model. This geometric approximation error is passed onto PSIM as the quadratic nodes are placed exactly between the edge nodes as opposed to on the surface of the geometry. This indicates a potential area of improvement for future implementations of PSIM as it should be possible to not just interpolate a displacement field but to use spline fitted mid-side node position for surface elements of curved geometry.

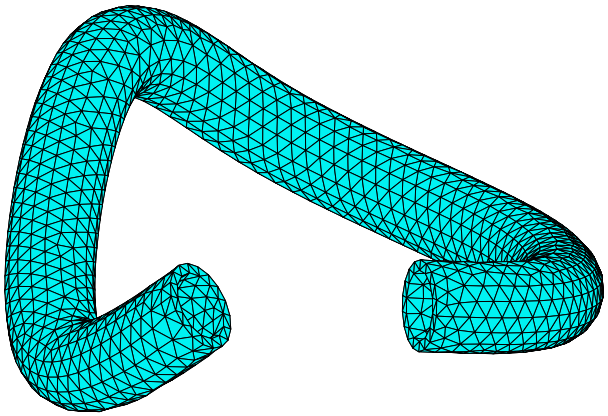

FIGURE 15. Non-Axisymmetric Incomplete Inflated Torus

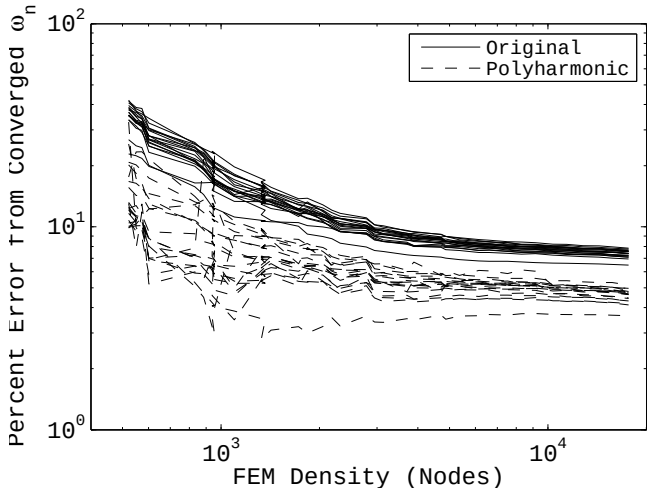

FIGURE 16. Convergence Study Comparing Original and Interpolation Based Eigenvalues

These results demonstrate again that the interpolated result is dependent on the accuracy of the original solution. While the eigenvalues computed from the Rayleigh quotient are closer to the quadratic results, the convergence rate, as in the previous examples, is identical to the original result. This relationship can be used to indicate when the model is nearing convergence as the relative difference between the original and interpolated solution is smaller when the original solution of the FEM is closer to the converged eigenfrequency. This is opposed to results from a convergence study which may falsely indicate that the model is converged due to a plateauing of eigenvalues. PSIM based SES shows the gain in model accuracy by utilizing higher order elements and will indicate FEM convergence based on the variation in eigenfrequencies from the original and interpolated solution.

CONCLUSION

In nearly all FEA problems an analytical solution is unavailable to the engineer and the computation of the best approximate solution invariably involves a convergence study. SES allows the engineer to obtain a significant improvement in eigenfrequency accuracy while introducing a measure of confidence on how the model would perform with a more refined mesh without actually refining the mesh or rerunning the analysis. The caveat is that SES is an *a posteriori* eigenfrequency refinement tool and cannot replace actual results from a higher order FEM since the interpolated results are still based on the solution of a lower order

FEM. However, since SES can provide better solution at the fraction of the computational cost it can indicate if model refinement is necessary even when it is infeasible or impossible to refine the model due to computational or modeling limitations.

While this research limited the application of SES to tetrahedral elements, it is well suited for mixed (i.e. tetrahedral, pyramidal, wedge, and/or hexahedral) meshes as the interpolation scheme is node rather than element based. Shape matrices are computed at the element level and therefore an updated eigenfrequency can be computed for a mixed element mesh at no additional programming or computational cost even for a FEM containing multiple element types. Future research will include the verification of SES for higher order and varied elements as well as evaluating the accuracy of interpolation results from cubic elements interpolated from quadratic hexahedral elements.

SES shows great promise of being able to provide the FEA engineer with a consistently higher accuracy eigenfrequency prediction at minimal computational cost. It should be noted that not only can SES be used for harmonic error estimation, but PSIM may also allow for the more accurate recovery of stress and strain within the FEM. This can be accomplished by interpolating existing FE results using clustered PSIM in order to accurately estimate maximal stress or other global maxima of field derivatives, and this will another topic of future research.

REFERENCES

[1] Bathe, K., 2007. *Finite Element Procedures*. Klaus-Jurgen Bathe.

[2] Heath, S., Slater, T., Mansfield, L., and Loftus, P., 1997. "Turbomachinery blade tip measurement techniques". In Proceedings 598 on Advanced Non-Intrusive Instrumentation for Propulstion Engines.

[3] Chan, Y. J., 2009. "Variability of blade vibration in mistuned bladed disks". PhD thesis, University of London.

[4] Roy, C. J., 2010. "Review of discretization error estimators in scientific computing". In 48th AIAA Aerospace Sciences Meeting.

[5] Walz, J. E., Fulton, R. E., and Cyrus, N. J., 1968. Accuracy and convergence of finite element approximations. Tech. rep., DTIC Document.

[6] Schmidt, H., Alber, T., Wehner, T., Blakytny, R., and Wilke, H., 2009. "Discretization error when using finite element models: Analysis and evaluation of an underestimated problem". *Journal of Biomechanics,* ***42***(12), pp. 1926 – 1934.

[7] Bauys, R., 1995. "Accuracy estimates in free vibration analysis". *Statyba,* ***1***(4), pp. 5–19.

[8] M. Ainsworth, T. J. O., 1997. "A posteriori error estimation in finite element analysis". *Computer Methods in Applied Mechanics and Engineering,* ***142***(12), pp. 1 – 88.

[9] Oh, H.-S., and Batra, R., 1999. "Application of zienkiewiczzhu's error estimate with superconvergent patch recovery to hierarchical p-refinement". *Finite Elements in Analysis and Design,* ***31***(4), pp. 273 – 280.

[10] Craig, A., Ainsworth, M., Zhu, J., and Zienkiewicz, O., 1989. "h and h-p version error estimation and adaptive procedures from theory to practice". *Engineering with Computers,* ***5***(3-4), pp. 221–234.

[11] Barlow, J., 1976. "Optimal stress locations in finite element models". *International Journal for Numerical Methods in Engineering,* ***10***(2), pp. 243–251.

[12] Zienkiewicz, O., Gago, J. D. S., and Kelly, D., 1983. "The hierarchical concept in finite element analysis". *Computers and Structures,* ***16***(14), pp. 53 – 65.

[13] Voltera, E., and Zachmanoglou, E. C., 1965. *Dynamics of Vibrations*. Charles E. Merrill Books, Inc.

[14] Yue, Z., and Robbins, D., 2003. "Rank deficiency in superconvergent patch recovery techniques with 4-node quadrilateral elements". *Communications in Numberical Methods in Engineering,* ***23***(1), pp. 1 – 10.

[15] Li, B., and Zhang, Z., 1999. "Analysis of a class of superconvergence patch recovery techniques for linear and bilinear finite elements". *Numerical Methods for Partial Differential Equations*.

[16] Rdenas, J. J., Tur, M., Fuenmayor, F. J., and Vercher, A., 2007. "Improvement of the superconvergent patch recovery technique by the use of constraint equations: the spr-c technique". *International Journal for Numerical Methods in Engineering,* ***70***(6), pp. 705–727.

[17] Gu, H., Zong, Z., and Hung, K. C., 2004. "A modified superconvergent patch recovery method and its application to large deformation problems". *Finite Elem. Anal. Des.,* ***40***(5-6), Mar., pp. 665–687.

[18] Beatson, R., Powell, M. J. D., and Tan, A. M., 2006. "Fast evaluation of polyharmonic splines in three dimensions". *IMA Journal of Numerical Analysis,* ***27***(3), pp. 427–450.

[19] MacQueen, J., 1967. Some methods for classification and analysis of multivariate observations.

[20] Castanier, M. P., and Pierre, C., 2002. "Using intentional mistuning in the design of turbomachinery rotors". *AIAA Journal,* ***40***(10), pp. 2077–2086.

[21] Petrov, E. P., and Ewins, D. J., 2003. "Analysis of the worst mistuning patterns in bladed disk assemblies". *Journal of Turbomachinery,* ***125***(4), pp. 623 – 631.